FINITE ELEMENT STUDIES OF TRANSIENT WAVE PROPAGATION

Mary Sansalone, Nicholas J. Carino, and Nelson N. Hsu

National Bureau of Standards
Gaithersburg, Maryland

INTRODUCTION

The National Bureau of Standards (NBS) has been working to develop a nondestructive test method for heterogenous solids using transient stress waves [1-5]. The method is referred to as the impact-echo method. The technique involves introducing a transient stress pulse into a test object by mechanical impact at a point and measuring the surface displacement caused by the arrival of reflections of the pulse from internal defects and external boundaries. Successful signal interpretation requires an understanding of the nature of transient stress wave propagation in solids containing defects. A primary focus of the NBS program is on using the finite element method to gain this understanding.

The purpose of this paper is to show the versatility and power of the finite element method for solving stress wave propagation problems, and to provide background information about the finite element program that was used to carry out the NBS studies. To achieve this purpose, this paper illustrates the use of the method to solve the following three problems: 1) stress and displacement fields produced by transient point impact on the surface of an elastic plate; 2) the interaction of transient stress waves with a planar disk-shaped void within an elastic plate; and, 3) stress fields produced by an ultrasonic transducer radiating into an elastic solid. The finite element results are compared to exact Green's function solutions for a point source on an infinite plate, experimentally obtained surface displacement waveforms for point impact on a plate containing a planar flaw, and photoelastic pictures of the stress fields produced by an ultrasonic transducer radiating into silica.

BACKGROUND

The finite element method is a general numerical technique for obtaining approximate solutions to the partial differential equations that arise from boundary value problems. The method involves dividing a continuum into a finite number of discrete parts - the finite elements. The discretized representation of the continuum is referred to as the finite element model. For stress analysis, the behavior of each element is described by a set of assumed functions which represent the variation of displacements within that element. Variational (or energy) principles are used to formulate force-displacement equations for the elements. These element equations are then used to construct the global equations which describe the behavior of the

entire continuum. Solution of these global equations gives the displacements at points in the element [6].

An explicit, two-dimensional (axisymmetric or plane strain), finite element code (DYNA2D), developed at Lawrence Livermore National Laboratory for solving finite-deformation, dynamic contact-impact problems [7-9], was used to perform the studies discussed in this paper. An input generator (MAZE) [10] was used to create the finite element model. A mini-computer with a virtual operating system, 8 MBytes of memory, and a floating point processor were used to carry out the analyses.

In DYNA2D, a continuum is divided into constant strain triangular and quadrilateral elements. Higher order elements (e.g., linear strain, quadratic strain) are not available in DYNA2D because they are computationally much more expensive in wave propagation applications than the use of constant strain elements. For a particular element type, the accuracy of the finite element solution is partly determined by element size. In wave propagation problems, the optimum element size depends on the geometry of the continuum and on the time-history of the dynamic loading.

In dynamic finite element analysis, numerical integration of the equations of motion must be carried out; DYNA2D uses the central difference method to perform this integration. The central difference method requires a small time step for numerical stability. This is not a drawback because wave propagation applications require the use of very small time steps to obtain an accurate solution. Numerical stability requires that the time step, h, meets the following criterion:

$$h \leq h_{max} = L/C_p \tag{1}$$

where L = shortest dimension of the element; and, C_p = P-wave velocity in the material. In DYNA2D, the time step is taken as 0.67 h_{max} unless the user specifies some other value. During an analysis, results are stored in data files at a time interval specified by the user.

A dynamic finite element analysis generates a large amount of data; therefore, an efficient and versatile post-processor is essential. An interactive, graphic, post-processor (ORION) [11] was used to process the results of the analyses. ORION allows the user to look at the results of an analysis in a variety of different ways. Full-field contour or vector plots or time-history plots can be obtained for a number of different parameters, including displacements, velocities, accelerations, stresses, and strains. Examples of several different types of data display are shown in this paper.

PLATE RESPONSE TO POINT IMPACT

Initial finite element studies were carried out using a solid plate so that the solutions could be compared to exact Green's function solutions for point impact on an infinite plate [3,4,12]. An axisymmetric, linear elastic analysis was performed for point impact on the surface of a 0.5-m thick, 1.5-m diameter, unsupported plate (Poisson's ratio of 0.2 and a P-wave velocity of 4000 m/s). The force-time history of the impact was modeled as a half-cycle sine curve with a duration of 25 microsec. The force was applied as a uniform pressure over the two elements at the center of the top surface of the plate.

Figure 1 illustrates two useful forms of data display: a vector plot of displacements, and a contour plot of stresses. In the vector plot, the magnitude and direction of the average nodal displacement of each element is indicated by a vector. Darker areas in the vector plot indicate areas

of larger displacements; thus, the various waves can be easily identified.
The right side of Figure 1(a) shows the vector displacement field through a
cross-section of the plate 125 microsec after the start of the impact. At
125 microsec, the P-wavefront arrives at the bottom of the plate. The posi-
tion of the P- and S-wavefronts are indicated on the left side of the figure.
Figure 1(b) shows a contour plot of minimum principal (compressive) stress
125 microsec after the start of the impact. Since a state of pure shear
stress is equivalent to a state of equal biaxial tension and compression, a
plot of minimum principal stress also shows the variation of stresses in
the S-wave. The letters A through E indicate the relative magnitude of the
stresses. The position of the P- and S-waves are indicated on the figure.
The magnitude of the stresses in the spherical P-wave are maximum near the
centerline of the plate. The stresses in the S-wave are small at the center
of the plate and become larger along rays located at increasing angles from
the center of the plate. Near the surface of the plate, the large amplitude
stresses caused by the Rayleigh (R) wave interfere with those produced by
the S-wave making it difficult to separate the stresses caused by each wave.
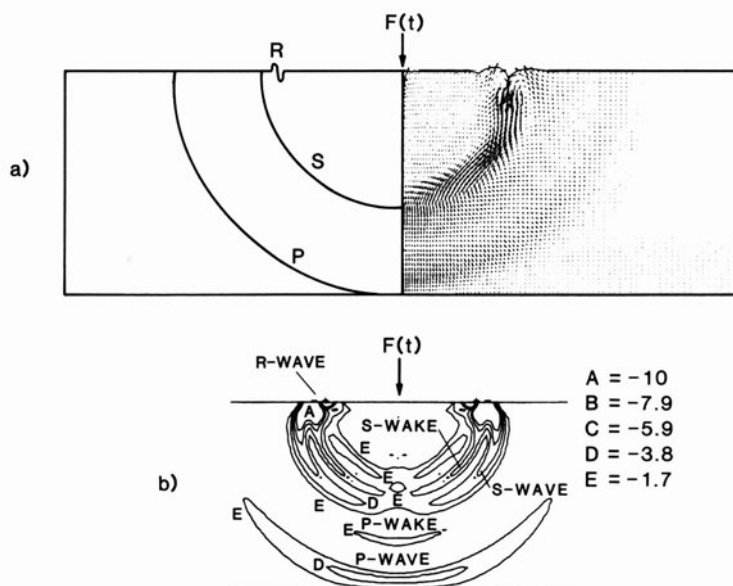

Fig. 1. Displacement and stress fields within a solid plate:
a) vector plot of displacements and the locations of
the wavefronts; and, b) minimum principal stress con-
tour plot.

The observed pattern of displacements and stresses in the P- and S-waves are similar to those expected based on the displacement fields produced by a harmonic point source [13]. However, in addition to the P-and S-wave radiation patterns, Figure 1(b) shows that in the region between the P- and S-waves there is a stress contour that resembles that in the P-wave; this disturbance is the "P-wake." In addition, there is a region of nonzero stresses trailing the S-wave that resemble the contours in the S-wave; this is the "S-wake." These wakes do not exist in the far-field solution for a harmonic point source. They were a significant finding of the finite element analysis and helped to explain previously unexplained features of surface displacement waveforms produced by a transient point source.

Figure 2 shows a comparison of a surface displacement waveform obtained from a Green's function solution (Figure 2(a)) with a surface displacement waveform obtained from the finite element analysis (Figure 2(b)). The test configuration and duration of the impact were the same for both solutions; in each case, the displacement was calculated 0.05 m away from the impact point. There is excellent agreement between the two waveforms. The only discrepancy appears following the R-wave, where the finite element waveform exhibits some spurious oscillations due to excitation of the zero-energy modes of the finite elements [7]. In this case, the zero-energy modes are excited by the element distortion caused by the rapid, large changes in displacement that occur in the R-wave. This "numerical ringing" does not affect the echo pattern due to the multiply reflected body waves.

The agreement between the waveforms shown in Figure 2 was achieved only after a correct finite element model was constructed. Convergence studies were carried out to determine the optimum element size for the constant strain quadrilaterals and the dynamic loading functions used in the linear elastic, plate analyses. The criterion for convergence was agreement between finite element displacement time-histories obtained at points on the top and bottom surfaces of a plate and the waveforms obtained at the same points by the Green's function solution for an infinite plate. For 0.25- to 0.5-m thick plates subjected to impacts with contact times of 25 to 30 microsec, rectangular elements with dimensions on the order of 0.02 times the plate thickness were found to give accurate results.
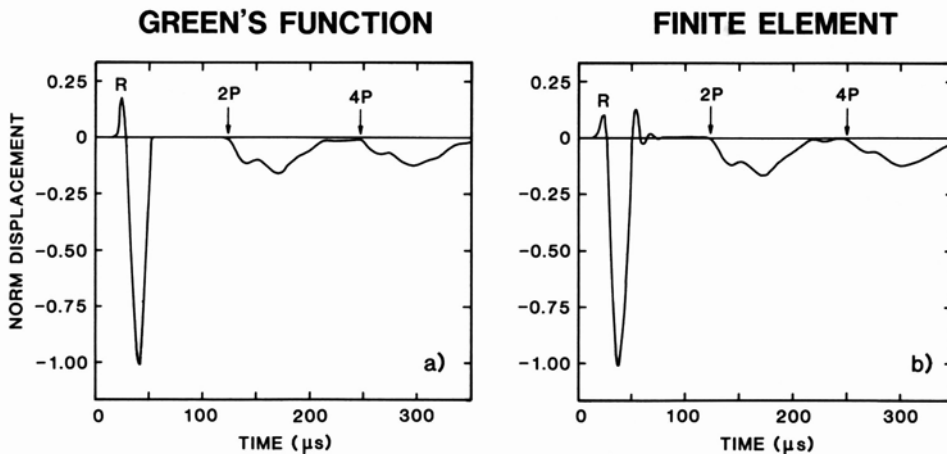

Fig. 2. Surface displacement waveforms: a) Green's function solution; and b) finite element analysis.

The next problems that were analyzed were point impacts on plates containing planar flaws [3,5]. The main focus of these studies was to determine the effects on stress and displacement fields in a plate and on surface displacement waveforms caused by diffraction of waves at the edges of a flaw. The capability of the finite element method to model diffraction at the edges of a flaw was established by comparing surface displacement waveforms obtained from analyses of an aluminum plate containing a flat-bottom hole to experimentally obtained waveforms. These comparisons are shown in Refs. [3,5]. Excellent agreement was found between the finite element and experimental waveforms. Thus, the finite element method was used to study various flaw geometries and impact conditions.

As an example, an analysis was performed for point impact on a 0.5-m thick, 1.5-m diameter plate (Poisson's ratio of 0.2 and P-wave velocity of 4000 m/s) containing a disk-shaped void. The void was 0.01-m thick and 0.1 m in diameter; it was located 0.25 m below the top surface of the plate. The contact time of the impact was 20 microsec. Figures 3(a)-(d) show contour plots of the minimum principal stresses in the plate at 65, 80, 95, and 125 microsec after the start of the impact.

The P-wavefront arrives at the flaw at 62.5 microsec, and is incident upon the edge of the flaw at 64 microsec. At 65 microsec, the stress contours in Figure 3(a) show that diffraction of the P-wave is occurring; the diffracted P-wavefront is beginning to emerge from the edge of the flaw. The diffracted P-wave forms a toroid with a circular cross-section. Rays emanating from the impact point and intersecting the edges of the flaw delineate the shadow zone beneath the flaw.

Figure 3(b) shows the stress contours at 80 microsec. At this time, the front of the reflected P-wave is just overlapping the front of the direct S-wave. The diffracted P-waves have overlapped in the center region of the plate, above and below the flaw. This figure clearly illustrates how diffraction causes large stresses to penetrate into the shadow zone.

At 95 microsec (Figure 3(c)), the P-wave has completely passed the flaw. The P-wave is formed by the overlapping of diffracted P-waves in the shadow zone and the original P-wave outside of the shadow zone.

Figure 3(d) shows the stress contours at 125 microsec. The various waves that are present at this time can be vividly seen in these contours. The P-wave reflected from the surface of the flaw has arrived at the top surface of the plate and the stress contour associated with this reflected wave is clearly seen. The S-wave produced by mode-conversion of the P-wave incident upon the flaw has traveled approximately 60 percent of the distance from the flaw to the top surface of the plate; the stress contour of this wave is also evident. Reflection and diffraction of the S-wave by the flaw have occurred, the P-wake has reformed below the flaw, and the P-wavefront is nearing the bottom surface of the plate.

Compare Figure 3(d) with Figure 1 which showed the stress field in a solid, 0.5-m thick plate at 125 microsec. In the plate containing the flaw, the stress pattern is much more complicated because of the interaction of the waves with the flaw. Notice that the stress field produced by the P-wave is similar to the stress field in the solid plate because diffraction allowed the P-wave to penetrate the shadow zone.

Displacement waveforms recorded near the point of impact at the top surface of a plate containing a flaw consist of displacements caused by waves reflected and diffracted from the flaw and waves reflected from the bottom

surface of the plate and subsequently diffracted by the flaw. The relative importance of the effects caused by each of these phenomena on displacement waveforms depends on the flaw geometry and the test conditions. Studies were carried out to better understand how waveforms are affected by these
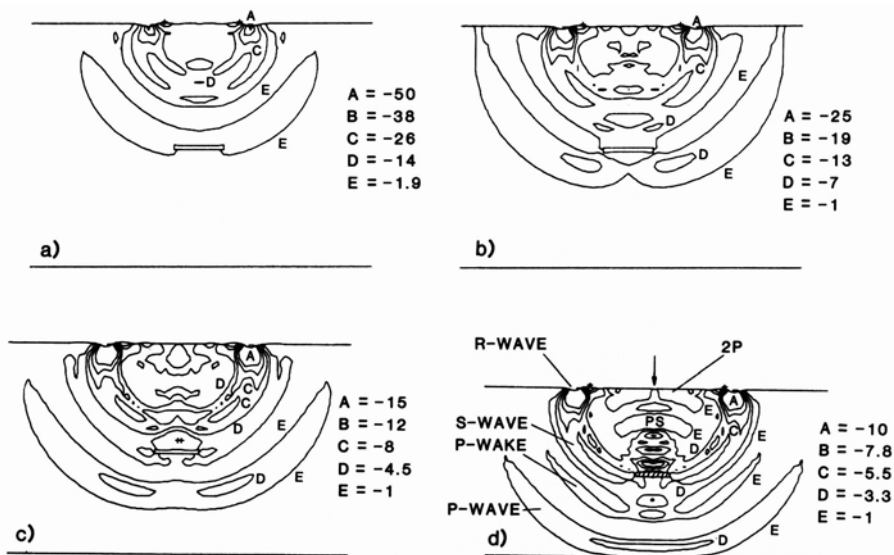

Fig. 3. Minimum principal stress contour plots occurring in a plate containing a disk-shaped flaw at various times after the start of the impact: a) 65; b) 80; c) 95; and, d) 125 microsec.

parameters. The variables examined included: the contact time of the impact; the diameter and depth of a flaw; and the test configuration, that is, the point where the displacement was recorded. The results of these studies are discussed in Ref. [3].

To show the versatility of the finite element method for studying wave propagation in solids, results obtained from an axisymmetric analysis of an idealized, 25.4-mm diameter transducer radiating into silica are presented. The input pulse produced by the transducer was simulated by applying a uniform pressure over a 25.4-mm diameter area at the center of a 140-mm diameter, 70-mm deep cylinder. The time-history of the pressure loading is shown in Figure 4. The loading is approximately a single cycle, damped sine curve; the duration of the loading was 1 microsec.

Figure 5(a) shows a stress contour plot of maximum shear stress obtained 11.5 microsec after the start of the input pulse. The P- and S-waves are labeled in this plot and letters A through E indicate the relative magnitude of stresses in the waves. The transducer can be though of as a multitude of point sources, each generating P- and S-waves and wakes. The radiation patterns produced by all these point sources are superimposed to produce the radiation pattern for the transducer. Notice that both the P- and S-waves are composed of regions of stresses directly below the transducer. In addition, the S-wave is also composed of a toroidal ring which is centered about the edge of the transducer. The largest stresses in the P-wave are an order of magnitude larger than those in the S-wave. This is in contrast to the stress pattern produced by a single point source (Figure 1(b)) in which the stresses in the S-wave are approximately the same or larger than those in the P-wave.

Figure 5(b) shows a photoelastic visualization 11.5 microsec after the start of an input pulse produced by a 1 MHz, broadband transducer radiating into silica [12]. The photoelastic technique relies on the difference in principal stresses (or shear stress). Therefore, Figure 5(b) can be compared directly to the shear stress contour plot that was shown in Figure 5(a). In Figure 5(b), the higher intensity of the illuminated P-wave indicates that the stresses are much higher in the P-wave than in the lower intensity S-waves. This is in agreement with the variation of stress contours in Figure 5(a). The agreement between the stress fields obtained by the finite element method and that obtained from photoelasticity is excellent.
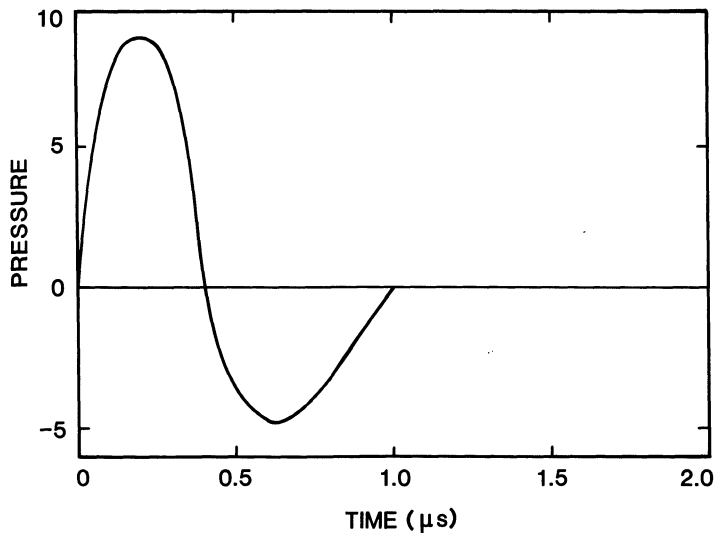

Fig. 4. Time-history of pressure loading for an idealized 25.4-mm diameter broadband transducer.

The results obtained from this finite element analysis can be used for much more than just visualization of the radiation pattern. Quantitative full-field information about stresses and displacements can be obtained, and finite element waveforms recorded on the top surface of a test specimen can be compared to experimentally obtained pulse-echo waveforms. A variety of input pulses can be modeled. Radiation patterns in specimens containing flaws can be studied. In particular, studies of standard reference blocks, such as the flat-bottom hole specimens, can be carried out.
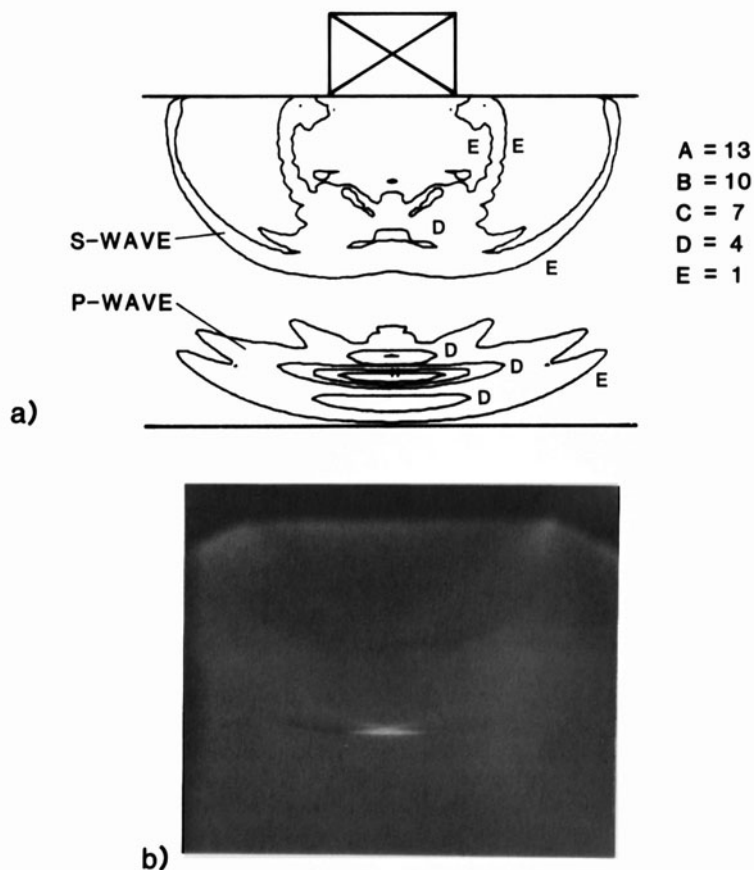

Fig. 5. Stress field produced by a broadband transducer radiating into silica: a) finite element shear stress contour plot; and, b) photoelastic visualization.

SUMMARY

These numerical studies were presented to illustrate the power of the finite element method as a tool for studying wave propagation in bounded solids subjected to arbitrary applied loads, boundary conditions, and containing flaws. In each of the examples presented in this paper, excellent agreement was obtained between finite element results and existing Green's function solutions for an infinite plate or experimental results. It is hoped that the work discussed in this paper and in Refs. [3-5] offers convincing evidence of the versatility of the finite element method for solving a wide variety of wave propagation problems for which there are presently no other solutions.

REFERENCES

1. N. J. Carino, M. Sansalone, and N. N. Hsu, J. Am. Conc. Inst. 83, 199 (1986).
2. N. J. Carino, M. Sansalone, and N. N. Hsu, Flaw Detection in Concrete by Frequency Spectrum Analysis of Impact-Echo Waveforms, in: "International Advances in Nondestructive Testing," W. J. McGonnagle, ed., Gordon & Breach Science Publishers, New York (1986).
3. M. Sansalone and N. J. Carino, "Impact-Echo: A Method for Flaw Detection in Concrete Using Transient Stress Waves," NBSIR 86- National Bureau of Standards, Gaithersburg, MD (1986).
4. M. Sansalone, N. J. Carino, and N. N. Hsu, ASME J. of App. Mech., submitted (Jan., 1986).
5. M. Sansalone, N. J. Carino, and N. N. Hsu, ASME J. of App. Mech., submitted (June, 1986).
6. R. H. Gallagher, "Finite Element Analysis, Fundamentals," Prentice-Hall, Englewood Cliffs (1975).
7. J. O. Hallquist, "A Procedure for the Solution of Finite-Deformation Contact-Impact Problems by the Finite Element Method," UCRL-52066, Lawrence Livermore Laboratory (1976).
8. G. J. Goudreau and J. O. Hallquist, Comp. Meth. in App. Mech. and Eng., 33, 725 (1982).
9. J. O. Hallquist, "User's Manual for DYNA2D - An Explicit Two-Dimensional Hydrodynamic Finite Element Code with Interactive Rezoning," Lawrence Livermore Laboratory (1984).
10. J. O. Hallquist, "User's Manual for MAZE: An Input Generator for DYNA2D and NIKE2D," Lawrence Livermore Laboratory (1983).
11. J. O. Hallquist, "User's Manual for ORION: An Interactive Post-Processor for the Analysis Codes NIKE2D, DYNA2D, and TACO2D," Lawrence Livermore Laboratory (1983).
12. N. N. Hsu, "Dynamic Green's Function of an Infinite Plate - A Computer Program," NBSIR 85-3234, National Bureau of Standards, Gaithersburg, MD (1985).
13. R. Roderick, Radiation Pattern from a Rotationally Symmetric Stress Source on a Semi-Infinite Solid, in: Ph.D. Thesis, Brown University, Providence (1951).
14. W. Sachse, N. N. Hsu, and D. G. Eitzen, Visualization of Transducer Produced Sound Fields in Solids, in: IEEE Ultrasonics Symposium Proceedings (1978).